Research Article | Vol. 26, No. 18 | 3 Sep 2018 | OPTICS EXPRESS 24154
Optics EXPRESS

Evaluation of gold layer configuration for plasmonic fiber grating biosensors

C. CAUCHETEUR,[1,*] M. LOYEZ,[2] Á. GONZÁLEZ-VILA,[1] AND R. WATTIEZ[2]

[1]*Electromagnetism and Telecommunication Department, University of Mons, Boulevard Dolez 31, 7000 Mons, Belgium*
[2]*Proteomics and Microbiology Department, University of Mons, Avenue du Champ de Mars 6, 7000 Mons, Belgium*
[*]*christophe.caucheteur@umons.ac.be*

Abstract: Gold-coated fiber Bragg gratings (FBGs) are nowadays a mature technology for lab-on-fiber sensing based on surface plasmon resonance (SPR) excitation. Tilted FBGs bring valuable assets such as easy light injection, remote operation in very small volumes of analytes and immunity to temperature fluctuations. Different gold configurations have been reported to date, without considering their relative performances in terms of biochemical sensing. In this work, we experimentally study the impact of the gold coating on the cladding mode distribution in the tilted FBG amplitude spectrum and subsequently on its sensitivity to cytokeratins used as biomarkers for cancer diagnosis. Some relevant configurations of gold coatings are produced and tested, relying on both the sputtering and electroless plating (ELP) processes. The obtained results confirm that the coating thickness and its roughness drive the biosensing performances. The experimental limit of detection for cytokeratins 17 sensing reaches 14 fM for the most sensitive configurations.

1. Introduction

Optical fiber refractometers coated by a thin metal film enable the excitation of surface Plasmon resonance (SPR). They constitute a miniaturized counterpart to the Kretschmann prism and are usually used for remote biochemical sensing purposes [1,2]. Surface plasmons are collective electrons oscillations at a metal-dielectric interface and are strongly sensitive to surrounding refractive index (SRI) changes at the metal surface. When bioreceptors are grafted on the gold-coated surface of an optical fiber, biochemical sensing is possible in very small volumes of analytes while being remotely operated, which is without equivalent for currently available commercial technologies [3].

For SPR excitation, the optical fiber guidance is locally modified to generate an evanescent lightwave at the cladding-metal interface. Two main kinds of configurations are usually produced to this aim. The first one consists in exposing the core-guided light to the surrounding medium by a local geometrical modification of the optical fiber (bending, etching, tapering, side-polishing, etc… [3–11]). The second one consists in photo-inscribing a refractive index modulation in the fiber core, usually in the form of long period fiber gratings (LPFGs) or tilted fiber Bragg gratings (TFBGs) [12–14].

TFBGs are short-period gratings that can be easily produced in telecommunication-grade single-mode optical fibers using the phase mask technique. For use in liquids, their grating planes are slightly angled (< 10°) with respect to the perpendicular to the optical fiber axis [15]. TFBGs yield a backward-going coupling of light to the cladding, where diameter is such that light is guided into numerous tens of cladding modes. This coupling provides a comb-like transmitted amplitude spectrum composed of narrowband cladding mode resonances. The self-coupling of the core mode also happens, yielding the Bragg resonance at the right end side of the spectrum, which can provide temperature decorrelation [16].

TFBGs excite surface plasmons at near-infrared wavelengths when they are coated with a thin gold layer and illuminated with P-polarized light, having its electrical field parallel to the metal interface [17]. A resolution to SRI changes better than 10^{-5} RIU (refractive index unit)

#341391 https://doi.org/10.1364/OE.26.024154
Journal © 2018 Received 2 Aug 2018; revised 23 Aug 2018; accepted 28 Aug 2018; published 31 Aug 2018

Optics EXPRESS

has been reported, both in liquids and gaseous media [18,19]. This feature has opened the way to the use of biofunctionalized gold-coated TFBGs for proteins and cells sensing [20–26].

TFBGs bring practical assets such as easy light injection, temperature fluctuations immunity and remote operation in very small volumes of analytes. To this aim, different metal configurations have been used so far [18,27–29], without considerations about their relative performances in terms of biosensing.

In this work, we study the impact of the coating on the cladding mode distribution in the TFBG transmitted amplitude spectrum and evaluate its influence on both the bulk sensitivity (grating response to SRI changes) and surface sensitivity (biosensing based on the antibody/antigen affinity) [11]. To this aim, several gold coating configurations were produced and tested on 1-cm-long 7° TFBGs, relying on both the sputtering and electroless plating (ELP) processes. They were biofunctionalized to detect cytokeratins (CK17), which are relevant biomarkers for cancer diagnosis.

In the following, section 2 focuses on the sensor fabrication while sections 3 and 4 present the results obtained for both bulk (volume) and surface sensing. It is important to mention that the performances obtained for volume refractometry do not necessarily drive those obtained for surface biosensing, as the latter is much more sensitive to the surface morphology rather than the penetration depth of the evanescent wave [11].

2. Sensor fabrication

2.1 Photo-inscription and interrogation of TFBGs

1-cm-long TFBGs were photo-inscribed in the core of hydrogen-loaded telecommunication-grade single-mode optical fiber (Corning SMF-28) using a 1090 nm period uniform phase mask and a frequency-doubled Argon-ion laser emitting at 244 nm (average output power of 50 mW). The phase mask was rotated in the plane perpendicular to the writing beam axis to create an external tilt angle of ~7° with respect to the perpendicular to the optical fiber longitudinal axis. This value ensures a strong coupling to cladding modes with an effective refractive index close to the one of water (1.315 in the telecommunication wavelength range). After their production, TFBGs were annealed at 100 °C during one day to remove the residual hydrogen and to stabilize their physical properties. The Bragg wavelength λ_{Bragg} corresponding to the self-coupling of the core mode and the wavelength at which the discrete coupling to the i^{th} cladding mode occurs $\lambda_{cladding,i}$ are given by the following set of phase matching conditions:

$$\lambda_{\text{Bragg}} = \frac{2n_{\text{eff,core}}\Lambda_G}{\cos\theta}. \tag{1}$$

$$\lambda_{\text{cladding,i}} = \left(n_{\text{eff,core}} + n_{\text{eff,cladding,i}}\right)\frac{\Lambda_G}{\cos\theta}. \tag{2}$$

where θ is the tilt angle. $n_{eff,core}$ and $n_{eff,cladding,i}$ are the effective refractive index of the core mode and the i^{th} cladding mode, respectively. Λ_g denotes the nominal grating period (cf. inset of Fig. 1) and is such that $\Lambda_g = \Lambda\cos\theta$ where Λ is the grating period along the axis of the fiber. Figure 1 depicts the typical transmitted amplitude spectrum of a 7° TFBG in air, featuring a spectral comb composed of several tens of narrowband cladding mode resonances at the left of the Bragg resonance.

An Amonics ASE source and a Yokogawa AQ6317C optical spectrum analyzer (OSA) were used to record the TFBG transmitted amplitude spectrum. A polarization controller was placed between the source and the TFBG to select the right input polarization state. Indeed, in the presence of a gold coating around the TFBG section, a splitting between P-polarized (TM and EH modes) and S-Polarized (TE and HE modes) resonances is usually obtained, as reported in [10,17–26]. Plasmonic effects are only reached for P-polarized lightwaves. When

Optics EXPRESS

used for volume or surface (bio)chemical sensing, the commonly adopted demodulation process of such gratings results in the tracking of the wavelength shift and/or amplitude variation of the most sensitive cladding mode resonance in the spectral comb [14]. The spectral position of this cladding mode resonance depends on the SRI value and on the overlay configuration.

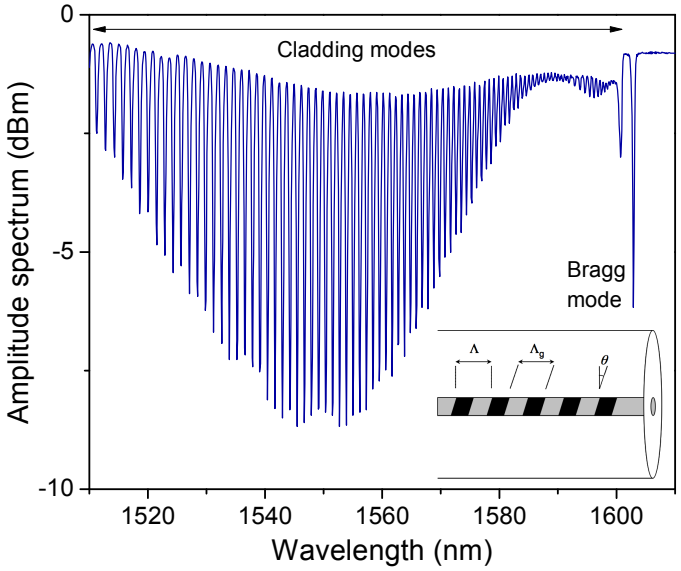

Fig. 1. Transmitted amplitude spectrum of a 1-cm-long 7° TFBG (inset: sketch of a TFBG).

2.2 Gold deposition

For the sputtering process, TFBGs were first cleaned with ethanol and then placed straight in the sputtering chamber (Leica EM SCD500 mounted with a 99.99% purity gold target), using an in-house developed support. The vacuum was obtained starting from dried ambient air. Gold of various thicknesses were deposited at room temperature by a double deposition with a fiber rotation of 180° in between. A built-in quartz micro-balance (Leica EM QSG100) installed in the sputtering chamber was used to control the deposited gold thickness.

For the electroless plating, TFBGs were first cleaned using a piranha solution (70% H_2SO_4: 30% H_2O_2) during 10 minutes and rinsed with deionized water. They were then immersed into APTMS ((3-aminopropyl)trimethoxysilane 97%) 1% in methanol during 20 minutes. After that, TFBGs were rinsed with methanol and dried at 80 °C during 15 minutes. They were placed into a commercial solution of 10 nm gold nanoparticles during 1 hour at room temperature. After rinsing with deionized water, they were finally immersed in the ELP plating bath containing 3 mM $HAuCl_4.3H_2O$ and 0.4 mM $NH_2OH.H_2SO_4$ in deionized water. TFBGs spectra were monitored in real time during the incubation to optimize the duration of the ELP process.

2.3 Biofunctionalization for cytokeratins sensing

Gold biofunctionalization first began by immersing the fibers into S_2-PEG_6-COOH (2 mM in ethanol) during 16 h at room temperature to form a self-assembled monolayer (SAM). The thiolated fibers were then smoothly washed using ethanol. After that, fibers were immersed in N-hydroxysuccinimide (NHS) 0.1 M/ 1-Ethyl-3-(3-dimethylaminopropyl)carbodiimide (EDC) 0.5 M diluted into miliQ water during 20 minutes at room temperature. Following this, the fibers were rinsed with PBS and immediately immersed in anti-CK17 antibodies solution, 20 µg/mL in PBS, pH 7.4 during 1h30 at room temperature. They were finally rinsed with phosphate buffer saline (PBS) buffer and blocked using 5% bovin serum albumin (BSA)

Optics EXPRESS

(w/v) in PBS during 1h30 at room temperature. After the process, OFs were rinsed again with PBS buffer and stored in dry conditions before use.

The functionalization of silica surfaces is slightly different. The optical fiber surface was first cleaned using a piranha solution and immersed into APTMS 1% in methanol during 20 minutes. Fibers were then placed in anti-CK17 antibodies solution (20 µg/mL) in PBS during 1h30 at room temperature. After this, optical fibers were placed into BSA 5% + PBS during 1h at room temperature, followed by a rinsing in PBS.

3. Bulk refractive index sensitivity

In this section, we report our experimental observations about the SRI sensitivity of different grating configurations. Four relevant surfaces are investigated in this work: bare, ~5 nm gold sputtered, ~35 nm gold sputtered and ~35 nm electroless-plated. The gold thickness was estimated using scanning electron microscopy (SEM). The choice for these specific thicknesses results from our previous work in this field [18] and from our wish to highlight the fundamentally differential behavior between sparse and continuous gold coatings. Ultrathin metal films (thickness < 10 nm) are prone to yield sensitivity enhancement. The latter does not result from a plasmonic effect, as recently verified in [30]. Such configurations are therefore particularly relevant to analyze in the case of biosensing, as an intermediate behavior between the ones of bare and plasmonic (metal thickness between ~30 and ~70 nm) configurations is most probable.

These configurations are immersed in salted solutions (mixture between distilled water and LiCl salt). The refractive index of these solutions is measured with an Abbe refractometer accurate to 10^{-4} RIU. Figure 2 gathers the obtained results. For each tested configuration, the transmitted amplitude spectrum recorded in salted solution (refractive index close to 1.37 at 1550 nm) is presented as well as the wavelength shift and amplitude variation of the most sensitive mode in this spectrum.

For bare gratings, it is well known that the most sensitive mode is the one above the cut-off mode, whose effective refractive index is slightly higher than the one of the surrounding medium [16]. It changes both in wavelength and in amplitude in response to slight SRI changes, as depicted in the inset of Fig. 2(a). Its wavelength shift yields a sensitivity of ~21 nm/RIU while its amplitude variation reaches ~147 dB/RIU, as obtained from a linear regression of the raw data (Fig. 2(b)).

In the case of ~5 nm gold-coated TFBGs, a clear polarization dependence is obtained around the cut-off wavelength, which corresponds to a wavelength splitting between P- and S-polarized modes. The spectrum depicted in Fig. 2(c) has been recorded with a polarization controller in such a way to record both orthogonal polarizations with almost equal amplitude. The inset of Fig. 2(c) reveals that the two polarizations behave differently. While S-polarized modes are almost insensitive to SRI changes, P-polarized ones exhibit an enhanced wavelength sensitivity compared to the unpolarized modes of bare gratings. The latter reaches ~33 nm/RIU, as depicted in Fig. 2(d). This results from the fact that only P-polarized modes can penetrate inside the gold layer, since their electric field is parallel to the gold surface. The amplitude sensitivity is however decreased (~54 dB/RIU), resulting from the splitting of the resonances, which decreases their peak-to-peak amplitude.

The third investigated case, corresponding to a gold thickness of ~35 nm deposited by sputtering, is well documented in the literature [10,17–26]. The gold layer is now sufficiently thick for SPR excitation with P-polarized cladding modes. Figure 2(e) depicts the corresponding transmitted amplitude spectrum, which features the typical SPR signature around 1565 nm. The SPR mode (the most attenuated in the spectrum) is usually tracked to follow large SRI changes, resulting in a wavelength sensitivity to SRI changes close to 550 nm/RIU. Its accurate tracking can no longer be made for small SRI variations limited to a few 10^{-4} RIU, as it corresponds to a strongly attenuated resonance that is difficult to reliably follow when shifts are very limited. Therefore, accurate and highly sensitive SRI sensing is

Optics EXPRESS

usually conducted by tracking the most sensitive mode located on the left edge of the SPR envelope, as shown in the inset of Fig. 2(e). Figure 2(f) shows that its refractometric sensitivity is ~55 nm/RIU for the wavelength shift while the amplitude variation peaks at 693 dB/RIU, a very high value offering the possibility to track very small SRI changes with a high resolution.

ELP gold coatings were finally investigated. As the process is conducted in solution, the TFBG spectral evolution can be monitored in real-time during the ELP, mainly to optimize the thickness of the deposited gold coating. From our observations, it turns out that the best-suited parameter to this aim is not the polarized transmitted amplitude spectrum but rather the polarization dependent loss (PDL) spectrum. The latter corresponds to the absolute value of the difference between orthogonally-polarized transmitted amplitude spectra [31]. The PDL of a bare grating displays a Gaussian shape for the cladding mode resonances spectrum, as shown in Fig. 2(g) (grey curve). From the start of the ELP process, the peak-to-peak amplitude of these resonances progressively vanishes until a clear narrowband signature related to the differential behavior between P- and S-polarized modes is obtained for a given duration of the ELP process. This peculiar signature, also shown in Fig. 2(g) (dark blue curve), is the sign that the process duration is optimum. The incubation time in this case is ~3 minutes. SEM characterizations revealed that the average gold thickness obtained in this case is ~35 nm while the surface coverage is ~75%. This configuration yields a bulk refractive index sensitivity decrease compared to bare TFBGs. Figure 2(h) shows that the wavelength sensitivity to SRI changes computed for an attenuated mode in the PDL spectrum (close to 1570 nm) is ~19 nm/RIU. The amplitude sensitivity has been computed to ~129 dB/RIU. The mode selected is the most sensitive one. Its localization is on the left edge of the PDL notch. Other configurations obtained for different incubation times (thus featuring different gold thicknesses) have been experimentally tested but, in the absence of interesting spectral feature, they do not provide interesting results.

Hence, our observations provide two main considerations about ELP: (1) gold coatings produced by this method do not yield SPR excitation and (2) the wavelength sensitivity to SRI changes is decreased compared to bare gratings. This is attributed to the morphology of the gold coating. Figure 3 shows SEM pictures of ~35 nm gold-sputtered and ~35 nm gold-electroless-plated configurations. While sputtering yields a relatively homogenous gold sheath (whatever the gold thickness), ELP provides an important granularity with some inhomogeneities, which we believe can enhance effects like localized SPR [32,33].

4. Surface biosensing

In this section, we focus on the biosensing capabilities of the different tested configurations that are now biofunctionalized, as explained in section 2.4. To this aim, gratings were first immersed in PBS supplemented by 10% of fetal bovin serum (FBS). Cytokeratins 17 were progressively added to obtain tenfold increments in the range 10^{-12} – 10^{-6} g/ml. Considering that the molecular weight of these commercial CK17 proteins is 73 kDa, the investigated range extends from 14 fM to 14 nM. First of all, it is important to mention that the proteins addition does not change the refractive index of the buffer measured by the Abbe refractometer. Figure 4 depicts the most sensitive cladding mode resonance of a functionalized ~35 nm gold-sputtered TFBG subject to increasing concentrations of CK 17. Amplitude variations of the resonance are visually much more important than the wavelength shifts. The latter badly reflect the response and are contained in a 15 pm wavelength range.

Optics EXPRESS

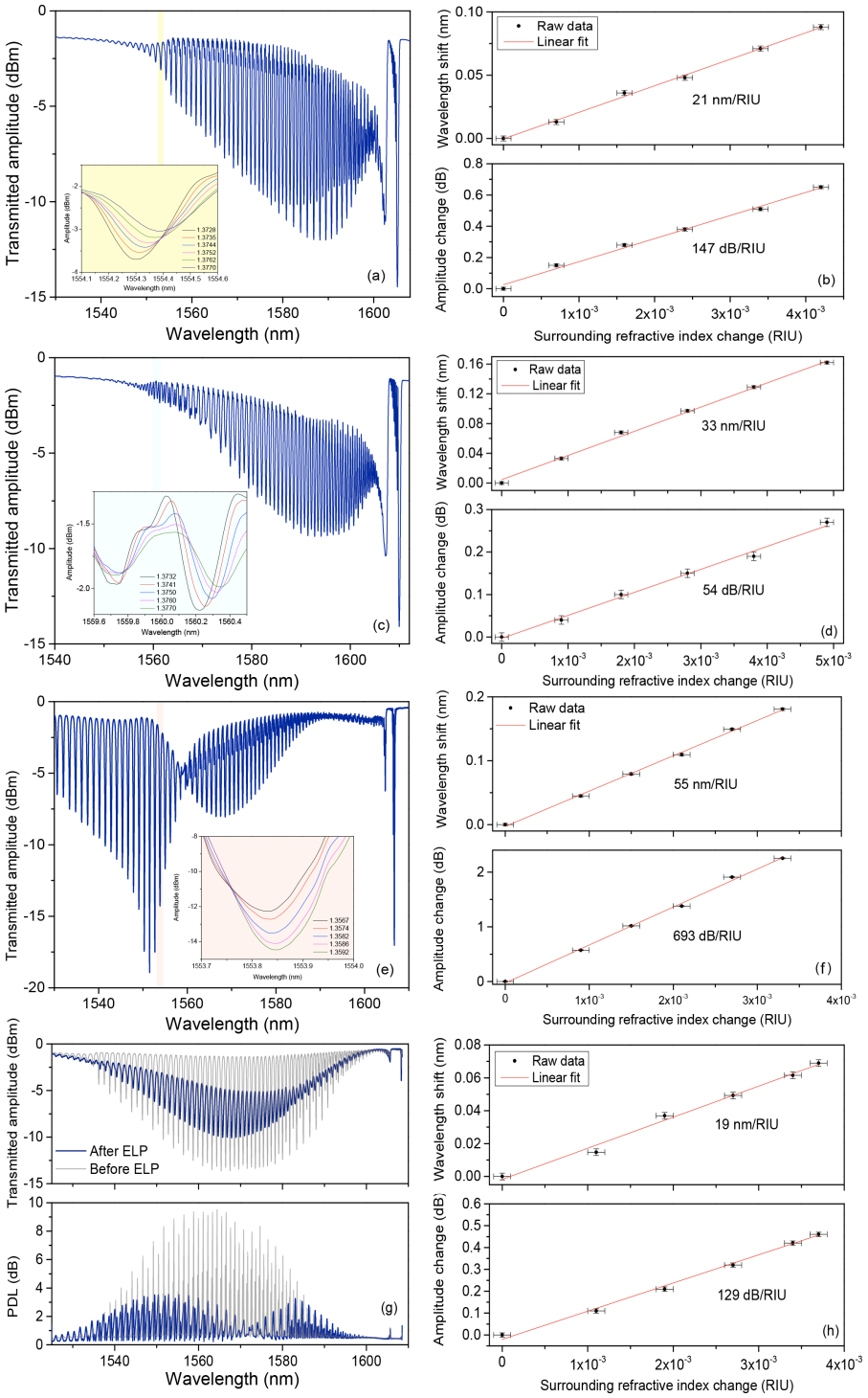

Fig. 2. Transmitted spectrum evolution for a bare grating (a), a ~5 nm gold-sputtered grating (c), a ~35 nm gold-sputtered grating (e) and a ~35 nm gold-electroless-plated grating (g). Corresponding SRI sensitivity of the most sensitive mode in their spectrum (b,d,f,h). Error bars represent the uncertainty on the SRI value (10-4 RIU) and on the wavelength (2 pm) and amplitude (0.01 dB) measurements.

Optics EXPRESS

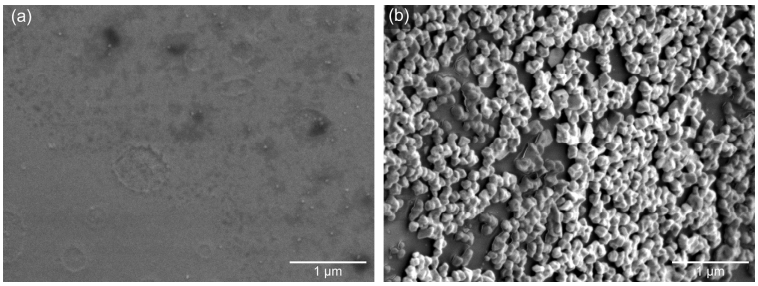

Fig. 3. SEM pictures of ~35 nm gold-sputtered (a) and ~35 nm gold-electroless-plated (b) optical fiber surfaces.

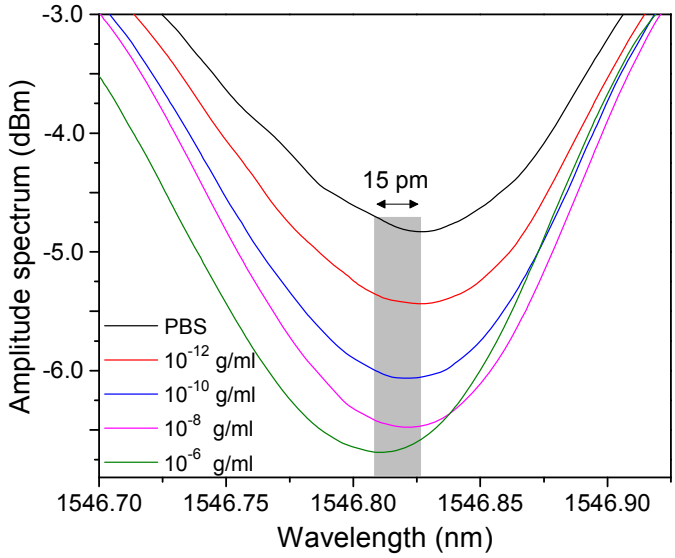

Fig. 4. Demodulation principle of TFBG biosensors. The displayed cladding mode resonance corresponds to the most sensitive mode of a ~35 nm gold-sputtered TFBG.

Hence, as done in all previous reports about the use of gold-coated TFBGs for biosensing [20–24], the most sensitive way to demodulate such biosensors remains to rely on amplitude variations of the most sensitive cladding mode resonance instead of wavelength shifts. Therefore, in the following, we will focus only on that parameter. Note that it is similar when the PDL spectrum is used in the case of electroless-plated gold coatings. In all cases, the Bragg resonance is used as a reference to avoid unwanted fluctuations linked to temperature changes or optical power variations.

Figure 5 depicts the relative peak-to-peak amplitude variations of the different tested configurations. Overall, it shows that bare gratings are weakly responsive, compared to gold-coated configurations. If we set to 0.05 dB the relative amplitude change required for proper CK17 sensing (grey part at the bottom of Fig. 5), the experimental limit of detection (LOD) of bare gratings is ~10^{-9} g/ml. The best option in terms of sensitivity remains the ~35 nm gold-sputtered configuration. Its amplitude variation is the highest and the LOD reaches ~10^{-12} g/ml. The ~35 nm gold-electroless-plated TFBG also behaves well with an LOD close to 10^{-11} g/ml. The ~5 nm gold-sputtered configuration shows an intermediate behavior between bare and ~35 nm gold-sputtered TFBGs. More interestingly, it presents the biggest amplitude variation between PBS and the lowest tested concentration of CK17. We attribute this to the sparsity of the ~5 nm gold coating, which provides an “hypersensitivity” to very small refractive index variations, as observed in [30] and as already reported for localized SPR

Optics EXPRESS

devices [32,33]. The actual LOD might be slightly lower than 10^{-12} g/ml. However, our experimental methodology did not allow us to verify this, as highly stable microfluidic systems are required to work with such very low analytes concentrations.

Hence, our experimental observations confirm that the biosensing performances can be tuned depending on the target application, by playing on the gold layer configuration.

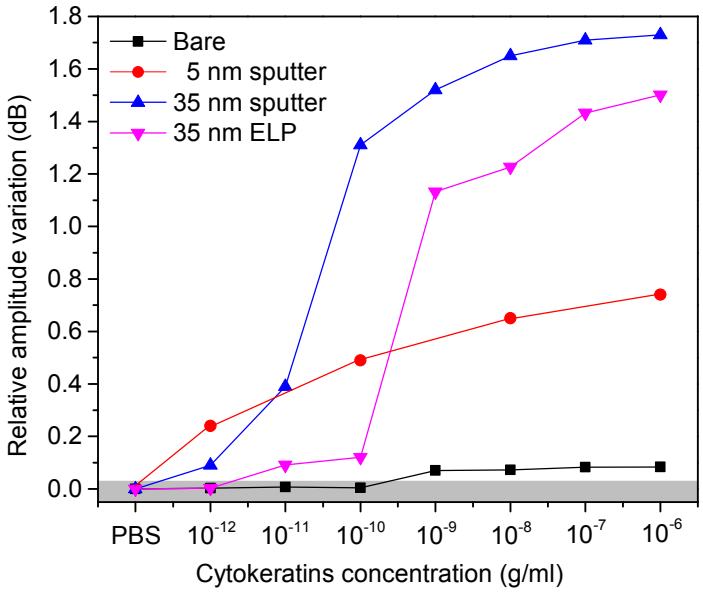

Fig. 5. Relative amplitude variations of the most sensitive mode of the different biofunctionalized TFBG configurations as a function of the CK17 concentration.

The table below (Table 1) summarizes the main characteristics of the TFBG configurations investigated in this work. According to our background in this field, we would like to emphasize that increasing the gold layer thickness beyond ~35 nm does not yield improved biosensing performances. Moreover, using more than 70 nm of gold prevents SPR excitation and makes the coated TFBGs useless for (bio)chemical sensing.

Table 1. Summary of the main characteristics of the tested gold-coated TFBGs configurations.

Configuration	Interrogation method	Volume SRI sensitivity	Experimental LOD for CK17 biosensing
Bare	Cut-off mode in unpolarized amplitude spectrum	~21 nm/RIU ~147 dB/RIU	~10^{-9} g/ml
5 nm sputtered	Most sensitive mode in polarized amplitude spectrum	~33 nm/RIU ~54 dB/RIU	≤10^{-12} g/ml
35 nm sputtered	SPR mode in P-polarized amplitude spectrum	~55 nm/RIU ~693 dB/RIU	~10^{-12} g/ml
35 nm ELP	Most sensitive mode in PDL spectrum	~19 nm/RIU ~129 dB/RIU	~10^{-11} g/ml

5. Conclusion

The purpose of this paper is to highlight the fundamentally different behavior of metal coatings used to enhance the performances of optical fiber refractometers and biosensors. In this work, we have produced and tested several relevant configurations of gold-coated TFBGs, obtained using both the sputtering and electroless plating techniques. We have analyzed the cladding modes distribution in the transmitted spectrum and studied their relative performances for both volume and surface sensing. Our experimental observations

Optics EXPRESS

confirm that the gold thickness and its relative granularity are important parameters to tune the biosensing performances. While TFBGs were used in this work, the experimental observations are certainly general and apply to other configurations such as long period fiber gratings, unclad/tapered/etched fibers and D-shaped fibers [34]. Therefore, we hope that this work can foster research activities towards enhanced surface sensitivity, which is highly relevant for biochemical sensing and immunosensing, not only with glass but also polymer optical fibers [10,11,35].

Funding

Fonds De La Recherche Scientifique (FNRS) (O001518F).

Acknowledgment

Fonds De La Recherche Scientifique (FNRS) (O001518F), Associate Researcher grant of C. Caucheteur, FRIA grants of M. Loyez and Á. González-Vila, EOS project Charming.

References

1. E. Kretschmann and H. Raether, "Radiative decay of non radiative surface plasmons excited by light," Z. Naturforsch. B **23**, 2135–2136 (1968).
2. R. Jorgenson and S. Yee, "A fiber-optic chemical sensor based on surface plasmon resonance," Sens. Actuators B Chem. **12**(3), 213–220 (1993).
3. J. Homola, "Optical fiber sensor based on surface plasmon excitation," Sens. Actuators B Chem. **29**(1–3), 401–405 (1995).
4. A. Trouillet, C. Ronot-Trioli, C. Veillas, and H. Gagnaire, "Chemical sensing by surface plasmon resonance in a multimode optical fiber," Pure Appl. Opt. **5**(2), 227–237 (1996).
5. M. H. Chiu, S. F. Wang, and R. S. Chang, "D-type fiber biosensor based on surface-plasmon resonance technology and heterodyne interferometry," Opt. Lett. **30**(3), 233–235 (2005).
6. R. Verma, A. Sharma, and B. Gupta, "Surface plasmon resonance based tapered fiber optic sensor with different taper profiles," Opt. Commun. **281**(6), 1486–1491 (2008).
7. Y. L. Lo, C. H. Chuang, and Z. W. Lin, "Ultrahigh sensitivity polarimetric strain sensor based upon D-shaped optical fiber and surface plasmon resonance technology," Opt. Lett. **36**(13), 2489–2491 (2011).
8. J. Pollet, F. Delport, K. P. F. Janssen, K. Jans, G. Maes, H. Pfeiffer, M. Wevers, and J. Lammertyn, "Fiber optic SPR biosensing of DNA hybridization and DNA-protein interactions," Biosens. Bioelectron. **25**(4), 864–869 (2009).
9. M. Navarrete, N. Díaz-Herrera, A. González-Cano, and Ó. Esteban, "Surface plasmon resonance in the visible region in sensors based on tapered optical fibers," Sens. Actuators B Chem. **190**, 881–885 (2014).
10. C. Caucheteur, T. Guo, and J. Albert, "Review of plasmonic fiber optic biochemical sensors: improving the limit of detection," Anal. Bioanal. Chem. **407**(14), 3883–3897 (2015).
11. F. Chiavaioli, C. A. J. Gouveia, P. A. S. Jorge, and F. Baldini, "Towards a uniform metrological assessment of grating-based optical fiber sensors: from refractometers to biosensors," Biosensors (Basel) **7**(4), 23 (2017).
12. T. Schuster, R. Herschel, N. Neumann, and C. G. Schäffer, "Miniaturized long-period fiber grating assisted surface plasmon resonance sensor," J. Lightwave Technol. **30**(8), 1003–1008 (2012).
13. B. R. Heidemann, I. Chiamenti, M. M. Oliveira, M. Muller, and J. L. Fabris, "Plasmonic optical fiber sensors: enhanced sensitivity in water-based environments," Appl. Opt. **54**(27), 8192–8197 (2015).
14. J. Albert, L. Shao, and C. Caucheteur, "Tilted fiber Bragg grating sensors," Laser Photonics Rev. **7**(1), 1–26 (2012).
15. C. Caucheteur and P. Mégret, "Demodulation technique for weakly tilted fiber Bragg grating refractometer," IEEE Photonics Technol. Lett. **17**(12), 2703–2705 (2005).
16. C. F. Chan, C. Chen, A. Jafari, A. Laronche, D. J. Thomson, and J. Albert, "Optical fiber refractometer using narrowband cladding-mode resonance shifts," Appl. Opt. **46**(7), 1142–1149 (2007).
17. Y. Shevchenko, C. Chen, M. A. Dakka, and J. Albert, "Polarization-selective grating excitation of plasmons in cylindrical optical fibers," Opt. Lett. **35**(5), 637–639 (2010).
18. C. Caucheteur, V. Voisin, and J. Albert, "Near-infrared grating-assisted SPR optical fiber sensors: design rules for ultimate refractometric sensitivity," Opt. Express **23**(3), 2918–2932 (2015).
19. C. Caucheteur, T. Guo, F. Liu, B.-O. Guan, and J. Albert, "Ultrasensitive plasmonic sensing in air using optical fibre spectral combs," Nat. Commun. **7**, 13371 (2016).
20. Y. Shevchenko, G. Camci-Unal, D. F. Cuttica, M. R. Dokmeci, J. Albert, and A. Khademhosseini, "Surface plasmon resonance fiber sensor for real-time and label-free monitoring of cellular behavior," Biosens. Bioelectron. **56**, 359–367 (2014).
21. V. Malachovská, C. Ribaut, V. Voisin, M. Surin, P. Leclère, R. Wattiez, and C. Caucheteur, "Fiber-optic SPR immunosensors tailored to target epithelial cells through membrane receptors," Anal. Chem. **87**(12), 5957–5965 (2015).

Optics EXPRESS

22. T. Guo, F. Liu, X. Liang, X. Qiu, Y. Huang, C. Xie, P. Xu, W. Mao, B. O. Guan, and J. Albert, "Highly sensitive detection of urinary protein variations using tilted fiber grating sensors with plasmonic nanocoatings," Biosens. Bioelectron. **78**, 221–228 (2016).
23. C. Caucheteur, T. Guo, and J. Albert, "Polarization-assisted fiber Bragg grating sensors: tutorial and review," J. Lightwave Technol. **35**(16), 3311–3322 (2017).
24. C. Ribaut, M. Loyez, J. C. Larrieu, S. Chevineau, P. Lambert, M. Remmelink, R. Wattiez, and C. Caucheteur, "Cancer biomarker sensing using packaged plasmonic optical fiber gratings: Towards in vivo diagnosis," Biosens. Bioelectron. **92**, 449–456 (2017).
25. Y. Zhang, F. Wang, S. Qian, Z. Liu, Q. Wang, Y. Gu, Z. Wu, Z. Jing, C. Sun, and W. Peng, "A novel fiber optic surface plasmon resonance biosensors with special boronic acid derivative to detect glycoprotein," Sensors (Basel) **17**(10), 2259 (2017).
26. T. Guo, Á. González-Vila, M. Loyez, and C. Caucheteur, "Plasmonic optical fiber-grating immunosensing: a review," Sensors (Basel) **17**(12), 2732 (2017).
27. W. Zhou, D. J. Mandia, S. T. Barry, and J. Albert, "Anisotropic effective permittivity of an ultrathin gold coating on optical fiber in air, water and saline solutions," Opt. Express **22**(26), 31665–31676 (2014).
28. D. Feng, W. Zhou, X. Qiao, and J. Albert, "High resolution fiber optic surface plasmon resonance sensors with single-sided gold coatings," Opt. Express **24**(15), 16456–16464 (2016).
29. Á. González-Vila, A. Ioannou, M. Loyez, M. Debliquy, D. Lahem, and C. Caucheteur, "Surface plasmon resonance sensing in gaseous media with optical fiber gratings," Opt. Lett. **43**(10), 2308–2311 (2018).
30. J. Albert, F. Liu, and V. Marquez-Cruz, "Hypersensitivity and applications of cladding modes of optical fibers coated with nanoscale metal layers," Sensors (Basel) **18**(5), 1518 (2018).
31. C. Caucheteur, Y. Shevchenko, L. Y. Shao, M. Wuilpart, and J. Albert, "High resolution interrogation of tilted fiber grating SPR sensors from polarization properties measurement," Opt. Express **19**(2), 1656–1664 (2011).
32. E. Petryayeva and U. J. Krull, "Localized surface plasmon resonance: nanostructures, bioassays and biosensing--a review," Anal. Chim. Acta **706**(1), 8–24 (2011).
33. J. Cao, M. H. Tu, T. Sun, and K. T. V. Grattan, "Wavelength-based localized surface plasmon resonance optical fiber biosensor," Sens. Actuators B Chem. **181**, 611–619 (2013).
34. F. Baldini, M. Brenci, F. Chiavaioli, A. Giannetti, and C. Trono, "Optical fibre gratings as tools for chemical and biochemical sensing," Anal. Bioanal. Chem. **402**(1), 109–116 (2012).
35. S. Cao, Y. Shao, Y. Wang, T. Wu, L. Zhang, Y. Huang, F. Zhang, C. Liao, J. He, and Y. Wang, "Highly sensitive surface plasmon resonance biosensor based on a low-index polymer optical fiber," Opt. Express **26**(4), 3988–3994 (2018).